FEBS Letters 414 (1997) 454–456 FEBS 19202

Pulsed EPR measurement of the distance between $P_{680}^{+\bullet}$ and $Q_A^{-\bullet}$ in photosystem II

Stephan G. Zech, Jens Kurreck, Hann-Jörg Eckert, Gernot Renger, Wolfgang Lubitz, Robert Bittl*

Max-Volmer-Institut für Biophysikalische Chemie und Biochemie, Technische Universität Berlin, Straße des 17. Juni 135, 10623 Berlin, Germany

Received 15 July 1997; revised version received 31 July 1997

Abstract Out-of-phase electron spin echo envelope modulation (ESEEM) spectroscopy was used to determine the distance between the primary donor radical cation $P_{680}^{+\bullet}$ and the quinone acceptor radical anion $Q_A^{-\bullet}$ in iron-depleted photosystem II in membrane fragments from spinach that are deprived of the water oxidizing complex. Furthermore, a lower limit for the distance between the oxidized tyrosine residue Y_Z of polypeptide D1 and $Q_A^{-\bullet}$ could be estimated by a comparison of data gathered from samples where the electron transfer from Y_Z to $P_{680}^{+\bullet}$ is either intact or blocked by preillumination in the presence of NH_2OH.

Key words: Cofactor distance; Oxygenic photosynthesis; Photosystem II; Pulsed electron paramagnetic resonance

1. Introduction

For photosystem II (PS II) of oxygenic photosynthesis a structural model based on X-ray or electron crystallography is not available at present. Structural parameters of PS II in particular distances between redox active species can, in principle, be obtained by the application of EPR techniques (see e.g. [1–4] and references therein). Several of the distance data derived from EPR spectroscopy, however, are of rather low precision with an error margin of 5–10 Å. Recently, a new application of pulsed EPR on light-induced radical pair (RP) states – out-of-phase ESEEM – has been used to gather distance information between the unpaired electron spins in RP within photosynthetic reaction centers [5–9] with a precision better than 0.5 Å. The method is based on the particular EPR properties of a spin polarized RP state generated by fast electron transfer from an excited singlet state [10]. Two groups have applied this method to determine the distance between the primary donor P_{700} and the phylloquinone acceptor A_1 in photosystem I (PS I) [6–8]. This distance is not yet available from the X-ray crystallographic model of PS I [11]. The values of 25.4 ± 0.3 Å and 25.3 ± 0.3 Å obtained for the distance between $P_{700}^{+\bullet}$ and $A_1^{-\bullet}$ for *Synechococcus elongatus* [6,7] and spinach [8], respectively, are in excellent agreement. Using the out-of-phase ESEEM technique on single crystals of PS I recently made it possible to derive three-dimensional structural information on the location of A_1 within the electron transfer chain of PS I [12].

In this study, the out-of-phase ESEEM method was applied to determine the distance between the primary donor P_{680} and the primary quinone acceptor Q_A in PS II. In order to eliminate problems arising from an incomplete cyclic electron flow in PS II under repetitive excitation at cryogenic temperatures, the out-of-phase ESEEM experiments were performed at room temperature using a flow system. This approach ensures a stable yield of the RP state $P_{680}^{+\bullet}Q_A^{-\bullet}$ by continuously refreshing the sample in the EPR resonator.

For EPR measurements on $Q_A^{-\bullet}$ in PS II a decoupling of $Q_A^{-\bullet}$ from the non-heme iron is necessary like in bacterial reaction centers (bRC). In bRC substitution of the Fe^{2+} by the diamagnetic Zn^{2+} is most widely used to achieve this decoupling [13]. For PS II several approaches have been used: (i) removal of the non-heme iron [14–16]; (ii) substitution by Zn^{2+} [17]; (iii) cyanide treatment to change the spin state of Fe^{2+} from $S=2$ to $S=0$ [18]; (iv) high pH treatment with an unknown reason for the decoupling [19]. In this study PS II preparations depleted of the non-heme iron have been used. A recent comparative investigation showed that iron-depleted samples retain the native function and structure better than the cyanide treated PS II membrane fragments [20]. The experimental results yield the distance between $P_{680}^{+\bullet}$ and $Q_A^{-\bullet}$ as well as an estimate for the distance between the oxidized tyrosine residue $Y_Z^{ox\bullet}$ and $Q_A^{-\bullet}$.

2. Materials and methods

2.1. Preparation of iron-depleted PS II membrane fragments

PS II membrane fragments were prepared according to Berthold et al. [21] with some modifications as described in Völker et al. [22]. Removal of the non-heme iron was performed as in MacMillan et al. [15]: mildly trypsinized PS II membrane fragments were incubated with 1,10-phenanthroline and lithium perchlorate. Subsequently conalbumin was added. For complete extraction of the iron, a second treatment with 1,10-phenanthroline, lithium perchlorate and conalbumin was necessary [16]. After the final centrifugation step the samples were resuspended in 20 mM MES/NaOH pH 6.5, 10 mM NaCl and 30% sucrose to chlorophyll concentrations of about 5 mM. They were frozen in small aliquots in liquid nitrogen and stored at −80°C until use. Removal of the non-heme iron was confirmed by measurements of the flash induced changes of the fluorescence quantum yield with home built equipment [23] as described in Kurreck et al. [16]. For measurements at pH 9 the samples were washed in a medium containing 50 mM Tris-HCl pH 9.0 and 10 mM NaCl. At pH 9.0 and room temperature the reduction of $P_{680}^{+\bullet}$ by Y_Z takes place with a time constant of less than 2 μs according to measurements of absorption changes at 830 nm (data not shown).

2.2. Donor side inhibition

The reduction of $P_{680}^{+\bullet}$ by Y_Z in the iron depleted PS II membrane

*Corresponding author. Fax: (49) (30) 314-21 122.
E-mail: bittl@pair.chem.TU-Berlin.DE

Abbreviations: bRC, bacterial reaction center; EPR, electron paramagnetic resonance; ESEEM, electron spin echo envelope modulation; MES, 2-(*N*-morpholino)ethanesulfonic acid; PS II, photosystem II; P_{680}, primary donor of PS II; Q_A, primary plastoquinone acceptor of PS II; RP, radical pair; SFT, sine Fourier transform; Y_Z, redox active tyrosine residue of polypeptide D1

PII S0014-5793(97)01054-5

fragments was blocked by preillumination in the presence of hydroxylamine (NH_2OH) [24]. Samples diluted to a chlorophyll concentration of 400 μM in 10 ml (final volume) buffer (containing 20 mM MES/NaOH pH 6.5 and 10 mM NaCl) were illuminated with strong white light (425 W m^{-2}) for 20 s in the presence of 1 mM $K_3Fe(CN)_6$ and 3 mM NH_2OH while stirring on ice. The reaction was stopped by 10-fold dilution with ice-cooled buffer. Afterwards the samples were washed twice. The inhibition of the electron transfer from Y_Z to $P_{680}^{+\bullet}$ was confirmed by measuring the kinetics of the $P_{680}^{+\bullet}$ rereduction via flash-induced absorption changes at 830 nm as described in Eckert et al. [25] (data not shown).

2.3. EPR spectroscopy

The pulsed EPR spectrometer with laser excitation, data acquisition and data processing has been described previously [7]. For the room temperature experiments presented here a continuous sample flow system consisting of a quartz capillary with 3 mm outer and 1 mm inner diameter centered in the dielectric ring resonator, 0.5 mm teflon tubing and a peristaltic pump replaced the He flow cryostat. The sample reservoir was kept in the dark at 0°C. The total sample volume used was about 1.2 ml. The flow time through the whole system was about 30 s. Of the total sample volume a fraction of 40% was in the tubing of the flow system and the rest in the cooled reservoir. A precise determination of the sample temperature in the EPR resonator was impossible due to the warming of the sample in the tubing of the flow system and the heating effect of the laser and microwave irradiation. The loading of the resonator with the highly 'lossy' sample resulted in the requirement of microwave pulses of 16 ns and 32 ns in a $h\nu$-t-$\zeta/2$-τ-ζ pulse sequence with $\zeta \approx 130°$ [9] for maximum echo intensity at a microwave power of nominally 400 W.

3. Results and discussion

Fig. 1 shows the observed out-of-phase ESEEM for the PS II membrane fragments with inhibited electron transfer from Y_Z to $P_{680}^{+\bullet}$. The first microwave pulse of a $\zeta/2$-ζ pulse sequence was applied at $t = 800$ ns after the laser flash and leads to the formation of the RP state $P_{680}^{+\bullet}Q_A^{-\bullet}$ with a time constant of about 300 ps [26,27]. The lifetime of this state in iron-depleted PS II with inhibited electron transfer from Y_Z was measured to be about 1 ms. Therefore, from the lifetime of the RP state the echo modulation signal shown in Fig. 1A can be assigned to the RP state $P_{680}^{+\bullet}Q_A^{-\bullet}$. The principal value $D = -135 \pm 4$ μT of the dipolar interaction and the value $J = 1 \pm 0.5$ μT for the isotropic exchange interaction between the unpaired spins on $P_{680}^{+\bullet}$ and $Q_A^{-\bullet}$ were obtained from simulation of the sine Fourier transforms (SFT) of the out-of-phase ESEEM on the basis of the theoretical model for out-of-phase ESEEM [10] as shown in Fig. 1B. The value of D corresponds to a distance between the two unpaired electron spins of 27.4 ± 0.3 Å in the point dipole approximation. This approximation is well satisfied as has been shown for the RP state $P_{865}^{+\bullet}Q_A^{-\bullet}$ in the bRC of *Rhodobacter sphaeroides* where the out-of-phase ESEEM yielded a distance between $P_{865}^{+\bullet}$ and $Q_A^{-\bullet}$ of 28.4 ± 0.3 Å, which is in excellent agreement with a distance between P_{865} and Q_A of 28.3 Å from the X-ray structure [28].

To further corroborate the assignment of the observed out-of-phase ESEEM to the RP state $P_{680}^{+\bullet}Q_A^{-\bullet}$, preparations of PS II were analyzed that are competent to reduce $P_{680}^{+\bullet}$ by Y_Z. In this sample the time constant for electron transfer from Y_Z to $P_{680}^{+\bullet}$ depends on the pH. A value of about 15 μs is observed at pH 6.5. Measurements on such samples at pH 6.5 resulted in echo modulation patterns indistinguishable within the signal/noise ratio from the one shown in Fig. 1A. Under these conditions the electron transfer from Y_Z to $P_{680}^{+\bullet}$ is slow compared with the time scale of our measurement and, therefore, results identical to those of samples with blocked electron transfer from Y_Z were found. In order to obtain further information, experiments were performed at pH 9.0 where the reduction of $P_{680}^{+\bullet}$ by Y_Z is faster than 2 μs. Thus, under these conditions electron transfer from Y_Z to $P_{680}^{+\bullet}$ takes place within the time scale of our measurements. Using a shorter delay time $t = 50$ ns between the laser pulse and the first microwave pulse, an out-of-phase ESEEM pattern is recorded which closely resembles that observed at pH 6.5. Fig. 2 shows the corresponding SFT as trace A. Increasing the delay time t strongly affects the observed out-of-phase ESEEM patterns. This is shown in Fig. 2 by the SFT of ESEEM patterns obtained with $t = 800$ ns and $t = 1200$ ns in traces B and C, respectively. A clear shift of the most prominent peak in the SFT around $|\nu_{max}| \approx 2$ MHz (indicated as a solid line) to lower frequencies (dashed line) with increasing delay is visible. This shift reflects the increasing contribution of the RP state $Y_Z^{ox\bullet}Q_A^{-\bullet}$ to the ESEEM patterns. The decrease of the frequency ν_{max} with highest amplitude in the SFT implies that the distance between the unpaired spins in the RP state $Y_Z^{ox\bullet}Q_A^{-\bullet}$ is larger compared to that of the state $P_{680}^{+\bullet}Q_A^{-\bullet}$. Unfortunately, the decreasing echo intensity with increasing delay time t does

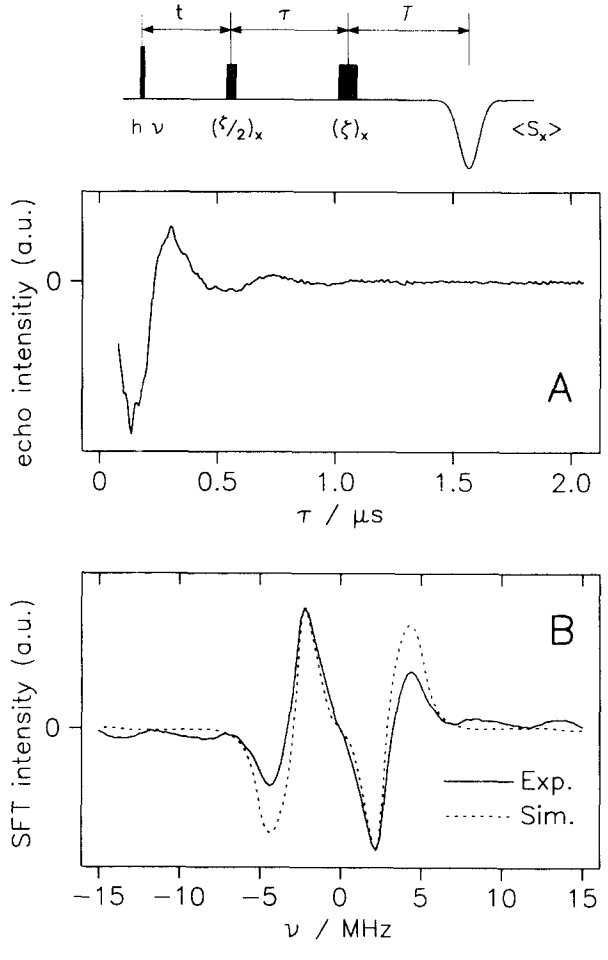

Fig. 1. Out-of-phase ESEEM of iron-depleted PS II membrane fragments with blocked electron transfer from Y_Z to $P_{680}^{+\bullet}$ measured near room temperature using the pulse sequence shown at the top with $t = 800$ ns. The recorded τ dependence is shown in part A. Part B shows the sine Fourier transforms (SFT) of the experimantal data of A (solid line) after reconstruction of the spectrometer deadtime [7] together with a numerical simulation (dotted line). The pulse scheme used for this experiment is shown at the top.

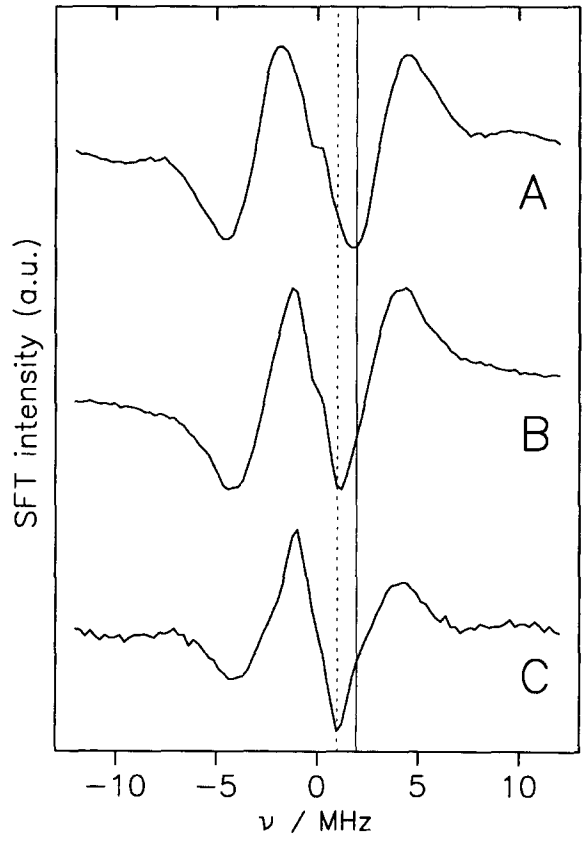

Fig. 2. Sine Fourier transforms (SFT) of the out-of-phase ESEEM observed for iron depleted PS II membrane fragments competent in electron transfer from Y_Z to $P_{680}^{+\bullet}$. Traces A, B, and C correspond to delay times $t = 50$, 800, and 1200 ns (see Fig. 1 top). The solid and dotted lines indicate the shift of the frequency with maximal intensity ν_{max}.

not permit an unambiguous conclusion that the value for ν_{max} observed at $t = 1200$ ns is the limit for complete reduction of $P_{680}^{+\bullet}$. This problem, and the missing theoretical treatment of out-of-phase ESEEM for a sequence of two consecutive RP states, prevents a direct interpretation of the data shown in Fig. 2 in terms of a precise distance between $Y_Z^{ox\bullet}$ and $Q_A^{-\bullet}$. However, a simulation of the central part of Fig. 2C around the frequency ν_{max} can be used to give a lower estimate for the distance between $Y_Z^{ox\bullet}$ and $Q_A^{-\bullet}$ of 32 Å.

4. Conclusion

Using the out-of-phase ESEEM spectroscopy on the RP states $P_{680}^{+\bullet}Q_A^{-\bullet}$ and $Y_Z^{ox\bullet}Q_A^{-\bullet}$ in iron depleted PS II preparations allowed a determination of the distance $r_{PQ} = 27.4 \pm 0.3$ Å between $P_{680}^{+\bullet}$ and $Q_A^{-\bullet}$. This result has been obtained for iron depleted PS II preparations with inhibited electron transfer from Y_Z as well as for samples which are competent in electron transfer from Y_Z at pH 6.5 showing slow reduction of $P_{680}^{+\bullet}$. The accelerated electron transfer from Y_Z to $P_{680}^{+\bullet}$ at pH 9.0 in non-inhibited samples provided the possibility to further study the effect of the reduction of $P_{680}^{+\bullet}$ by $Y_Z^{ox\bullet}$ on the out-of-phase ESEEM. The resulting altered ESEEM patterns have been used to give a lower limit for the distance r_{YQ} between $Y_Z^{ox\bullet}$ and $Q_A^{-\bullet}$ of $r_{YQ} > 32$ Å.

Acknowledgements: The authors thank F. Reifarth and G. Christen (TU Berlin) for time-resolved fluorescence measurements. Stimulating discussions and collaboration in transient EPR experiments on PS II with A. van der Est and D. Stehlik (FU Berlin) are gratefully acknowledged. This work has been supported by Deutsche Forschungsgemeinschaft (Sfb 312, TP A2/A4), a graduate fellowship to S.G.Z. (NaFöG) and Fonds der Chemischen Industrie (to W.L. and G.R.).

References

[1] Un, S., Brunel, L.-C., Brill, T.M., Zimmermann, J.-L. and Rutherford, A.W. (1994) Proc. Natl. Acad. Sci. USA 91, 5262.
[2] Gilchrist, M.L., Ball, J.A., Randall, D.W. and Britt, R.D. (1995) Proc. Natl. Acad. Sci. USA 92, 9545.
[3] Hara, H., Kawamori, A., Astashkin, A.V. and Ono, T.-a. (1996) Biochim. Biophys. Acta 1276, 140.
[4] Deligianakis, Y. and Rutherford, A.W. (1996) Biochemistry 35, 11239.
[5] Dzuba, S.A., Gast, P. and Hoff, A.J. (1995) Chem. Phys. Lett. 236, 595.
[6] Zech, S.G., Lubitz, W. and Bittl, R. (1996) Ber. Bunsenges. Phys. Chem. 100, (12) 2041.
[7] Bittl, R. and Zech, S.G. (1997) J. Phys. Chem. B 101, 1429.
[8] Dzuba, S.A., Hara, H., Kawamori, A., Iwaki, M., Itoh, S. and Tsvetkov, Y.D. (1997) Chem. Phys. Lett. 264, 238.
[9] Zech, S.G., Bittl, R., Gardiner, A.T. and Lubitz, W. (1997) Appl. Magn. Reson. (submitted).
[10] Salikhov, K.M., Kandrashkin, Y.E. and Salikhov, A.K. (1992) Appl. Magn. Reson. 3, 199.
[11] Krauß, N., Schubert, W.-D., Klukas, O., Fromme, P., Witt, H.T. and Saenger, W. (1996) Nature Struct. Biol. 3, 965.
[12] Bittl, R., Zech, S.G., Fromme, P., Witt, H.T. and Lubitz, W. (1997) Biochemistry (submitted).
[13] Debus, R., Feher, G. and Okamura, M. (1984) Biochemistry 25, 2276.
[14] Klimov, V., Dolan, E.E.S. and Ke, B. (1980) Proc. Natl. Acad. Sci. USA 77, 7227.
[15] MacMillan, F., Lendzian, F., Renger, G. and Lubitz, W. (1995) Biochemistry 34, 8144.
[16] Kurreck, J., Garbers, A., Reifarth, F., Andréasson, L.-E., Parak, F. and Renger, G. (1996) FEBS Lett. 381, 53.
[17] Akabori, K., Kuroiwa, S. and Toyoshima, Y. (1992) in: N. Murata (Ed.), Research in Photosynthesis, Proceedings of the IXth International Congress on Photosynthesis, Nagoya, Japan, August 30–September 4, 1992, Vol. II, pp. 123–126. Kluwer, Dordrecht.
[18] Sanakis, Y., Petrouleas, V. and Diner, B.A. (1994) Biochemistry 33, 9922.
[19] Deligianakis, Y., Jegerschöld, C. and Rutherford, A.W. (1997) Chem. Phys. Lett. 270, 564.
[20] Renger, G., Kurreck, J., Haag, E., Reifarth, F.,, Bergmann, A., Parak, F., Garbers, A., MacMillan, F., Lendzian, F. and Lubitz, W. (1997) in: A.X. Trautwein (Ed.), Bioinorganic Chemistry, pp. 160–177. VCH, Weinheim.
[21] Berthold, D., Babcock, G. and Yocum, C. (1981) FEBS Lett. 134, 231.
[22] Völker, M., Ono, T., Inoue, Y. and Renger, G. (1985) Biochim. Biophys. Acta 806, 25.
[23] Gleiter, H.M., Ohad, N., Hirschberg, J., Fromme, R., Renger, G., Koike, H. and Inoue, Y. (1990) Z. Naturforsch. 45c, 353.
[24] Ford, R.C. and Evans, M.C.W. (1985) Biochim. Biophys. Acta 807, 1.
[25] Eckert, H.-J., Wydrzynski, T. and Renger, G. (1988) Biochim. Biophys. Acta 932, 240.
[26] Eckert, H.-J., Wiese, N., Bernarding, J., Eichler, H.-J. and Renger, G. (1988) FEBS Lett. 240, 153.
[27] Bernarding, J., Eckert, H.-J., Eichler, H.J., Napiwotzki, A. and Renger, G. (1994) Photochem. Photobiol. 59, 566.
[28] Ermler, U., Fritzsch, G., Buchanan, S.K. and Michel, H. (1994) Structure 2, 925.